View metadata, citation and similar papers at core.ac.uk
brought to you by CORE
provided by Ghent University Academic Bibliography

JOURNAL OF APPLIED PHYSICS 115, 17A333 (2014)

Characterizing local anisotropy of coercive force in motor laminations with the moving magnet hysteresis comparator

I. J. Garshelis[1,a)] and G. Crevecoeur[2]
[1]Magnova, Inc., Pittsfield, Massachusetts 01201, USA
[2]Department of Electrical Energy, Systems and Automation, Ghent University, Ghent 9000, Belgium

(Presented 7 November 2013; received 23 September 2013; accepted 20 November 2013; published online 27 February 2014)

Non oriented silicon steels are widely used within rotating electrical machines and are assumed to have no anisotropy. There exists a need to detect the anisotropic magnetic properties and to evaluate the local changes in magnetic material properties due to manufacturing cutting processes. In this paper, the so called moving magnet hyteresis comparator is applied to non destructively detect directional variations in coercive force in a variety of local regions of rotor and stator laminations of two materials commonly used to construct induction motors cores. Maximum to minimum coercive force ratios were assessed, varying from 1.4 to 1.7. © *2014 AIP Publishing LLC*. [http://dx.doi.org/10.1063/1.4866552]

Cores of most rotating electrical machines are assembled from laminations cut from sheets of non oriented (NO) silicon steels. It is well understood that these materials are only "notionally" free of crystalline texture,[1] hence there are in the literature numerous accounts of the consequential anisotropy in magnetic properties such as hysteresis loss and coercive force.[2] Detrimental effects of this anisotropy on the efficiency,[3] noise, vibration, and other operational features[4] of such machines have been measured, and analyzed.

It is also known that cutting sheet material deteriorates desirable magnetic properties in the edge regions,[5] and that the extent of these effects, while understandably dependent on the cutting technique, is also different in the rolling (RD) and transverse (TD) directions.[6] In typical stator and rotor laminations the volume density of cut affected material is significantly greater in "tooth" areas (i.e., between winding slots) than in the annular "back iron" areas. A need therefore exists for a measurement technique able to assess differences in the anisotropy of coercive force among such localized regions of actual laminations, rather than in standardized test samples. Detection of anomalous differences in coercive force anisotropy between "identical" samples, or between adjacent teeth in one sample, can inform on inconsistencies in the material or production processes, or changes in the condition of the tooling. The Moving Magnet Hysteresis Comparator (MMHC) has been shown[7,8] to provide a simple and sensitive non-destructive means for obtaining comparative coercive force measurements in *local* regions of sheet materials. This paper studies the local region's extent examined by the MMHC, and presents results from the use of this technique in the examination of different portions of rotor and stator laminations.

Conventional measurement methods subject the entire sample to a uniform, time varying magnetic field, whereas the MMHC excites only a relatively small region of the sample by exposure to the spatial magnetic field pattern surrounding a small permanent magnet (PM).[7] In a plane normal to the magnetic moment of the PM, both the pattern and intensity of this field have been shown to closely mimic those from a single dipole[7] of equal moment (m), located somewhat further from this plane than the nearest face of the PM. The distance from this dipole to the plane is called the gap (G). The PM, together with its "attached" field pattern is moved over the sample under test (SUT), in a straight line, at constant G, for a distance (typically 1–10G) called the "stroke" (S). The PM is moved first in the "forward" (F) direction, then in the reverse (R) direction, back to its starting position. In conventional methods, the (average) magnetization within the sample cross section is measured synchronously with the field; in the MMHC method the longitudinal component of the field (H) beneath the sample at the center of the stroke is measured, by a field sensing device (FS), synchronously with the PM position relative to the FS ($\pm x$), and recorded during both directions of PM motion. For each value of x (or just the value or values relevant to the measurement purpose) the *difference* in the fields measured during each direction of motion (i.e., $D(x) = H(x)_F - H(x)_R$) is calculated.

It is readily understood that $D(x)$ reflects the coercive force of the SUT.[7] The magnetization, $M(x)$, at points within the region affected by the moving PM field pattern has been shown to follow ascending and descending limbs of a major hysteresis loop during F and R motions, respectively. Thus, the same irreversible magnetization processes which separate these limbs, also distinguish the $M(x)_F$ and $M(x)_R$ patterns in the region affected by the PM field. Since $H(x) = H_{PM}(x) + H_S(x)$, where $H_{PM}(x)$ and $H_S(x)$ are the fields from the magnet and from the divergence of magnetization within the SUT respectively, and $H_{PM}(x)$ is the same in both directions, $D(x)$ is seen to reflect those same differences in the H–M characteristics which separate the two limbs of a hysteresis loop, a separation clearly quantified by coercive force, H_c.

H_c of samples which are homogeneous in dimensions, structure, and composition, throughout and near the region being scanned, can be expressed by the single difference at $x = 0$, i.e., $D(0)$.[7,8] Conventional methods report on "global" properties of the SUT, whereas the MMHC reports on H_c of

a)Electronic mail: ijgarsh@att.net.

 © 2014 AIP Publishing LLC

material only within the region "scanned" by the PM field. The boundary dimensions of this region derive from the basic parameters of the MMHC technique, i.e., m, G, S, the size and shape of the PM (which determine how closely its field mirrors that of a single dipole), and ultimately on H_c of the SUT relative to the peak intensity of the fields encountered during PM motion. For the "equivalent" dipole, the longitudinal field, $H = 3mxG/(x^2 + G2)^{5/2}$, from which $H_{peak} = \pm 0.8587m/G^3$ at $x = \pm 0.5G$, respectively.[7] Since the opposite polarity peak fields are distance G apart, during motion over a distance S, material within a region of length, $L = S–G$, will be exposed to the full range of available fields. We define this as the "local region" and note that it is symmetrically disposed around the FS location.

Identifying a width dimension, W, for the local region, using the same H_{peak} criteria is not possible, since as transverse distance (y) from the dipole axis increases, the effective gap becomes both larger and more inclined to the plane of the SUT. This has two consequences: a decrease in H_{peak} and an increase in distance between $+H_{peak}$ and $-H_{peak}$. Fig. 1 shows these changes to also occur in the field distribution from a real magnet. They combine to reduce the field gradient, dH/dx, the magnetization gradient dM/dx $\nabla \cdot M$ and the field arising from $\nabla \nabla \cdot M$. The material in which this field arises is also further from the FS ($\approx y$) thus contributing less to the signal. At locations off the dipole axis, there are also fields in the y direction, with peak amplitudes at $y = \pm 0.5G$. The presence of such fields clearly invalidates the single axis, ascending/descending limb model of the magnetization changes in the material where y exceeds $\approx 0.25G$. Finally, it is noted that the FS element is typically <1 mm wide and only detects longitudinal fields. In consideration of the foregoing, we assume $1\text{ mm} < W < 0.5G$.

PMs which are wider in the y than in the x direction act more like a linear array. The field intensity for such a PM has been shown[9] to be greatest at its center, notably smaller at its edges, and diminish ever more rapidly with increasing transverse distance from its edges. These features are quantitatively dependent on the PM size and shape. An example is seen in Fig. 1.

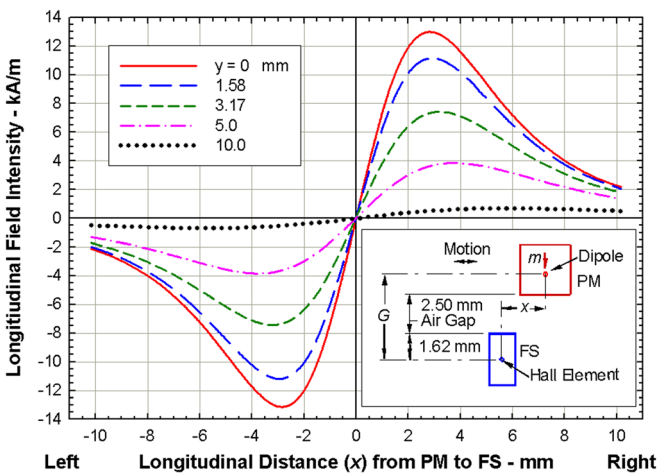

FIG. 1. Longitudinal field pattern from 3.175 mm cube PM at transverse distances (y) from the PM centerline and a 2.5 mm Gap between the PM face and FS. The inset illustrates the relation between distance G and the physical gap between opposing faces of the PM and FS.

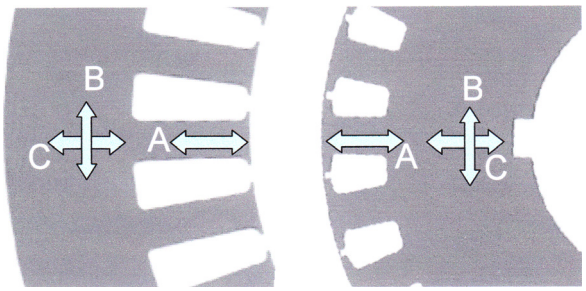

FIG. 2. Magnet strokes for Stator (left) and Rotor (right) laminations. "A": radial along a tooth; "B": tangential in back iron; "C": radial in back iron.

Stator and rotor laminations of coated AISI M36 and AISI M19, fully processed silicon steels intended for use in four pole induction motors were obtained from a major manufacturer. Four laminations of each material for each function were obtained (16 parts total). M36 parts were 0.635 mm thick (ASTM Type 64F210); M19: 0.356 mm thick (ASTM 36F155). Stators had 36 slots, outer diameter (OD) of 198 mm, inner diameter of 125 mm. The rotors: 28 slots, 25 mm OD, 50 mm ID, with a 6.35×3.0 keyway. The lamination under test (LUT) was mounted in a previously described MMHC apparatus,[7] modified to allow for manual rotation on its vertically oriented axis to fixed positions relative to each tooth. The axis could be positioned such that the magnet stroke in either radial or tangential directions would be approximately centered in the back iron region, or radially along the center of each tooth. See Fig. 2. The LUT was lightly clamped under a windowed (to allow for the magnet motion) aluminum plate to prevent any LUT deflection in response to the attractive force of the PM.

The PM was moved forward and back 3 times over its full stroke (20 mm) to stabilize the magnetization changes. It was then moved to the stroke center ($x = 0$) for the measurement of $H(x)_F$. Then back to the $x = 0$ position at which time $H(x)_R$ was acquired, and $D(0)$ calculated. A cube shaped, Grade 42, NdFeB magnet, 3.18 mm on each side, with a 2.5 mm air gap to the FS (Allegro Microsystems, 3515UA Hall Effect IC) was used for all of the tests. Plots of $D(0)$ at the angular position of the center of each tooth relative to an assumed RD at the tooth location for which $D(0)$ was a minimum, are shown in Figs. 3 and 4 for LUTs and PM stroke locations and orientations. $D(0)$ for each plot is normalized against its respective minimum value.

The results exhibit both novel content and unusual features when compared to analogous plots in the literature.[2] When considering roll induced anisotropy, angular ranges of 0°–90° or 180°–270° are from RD to TD, while 90°–180° and 270°–360° are TD to RD. The presented methodology enables local measurement of the relative coercive force at different locations within a single sample. The coercive force at each location is affected by both the roll induced crystal texture and the local deformations and residual stress distributions instilled during the lamination cutting process.

We first applied the MMHC onto the M19 and M36 materials resulting in the $D(0)$ measurements depicted in

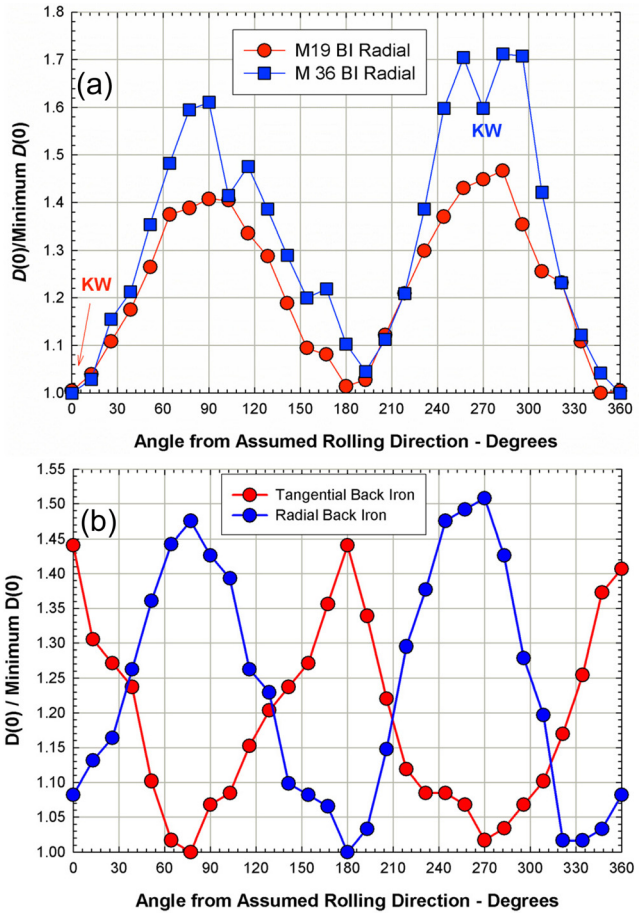

FIG. 3. (a) Comparison of $D(0)$ measured in the radial direction in the back iron regions of M19 and M36 rotor laminations. (b) Comparison of $D(0)$ measured in tangential and radial directions in the back iron region of M19 rotor lamination.

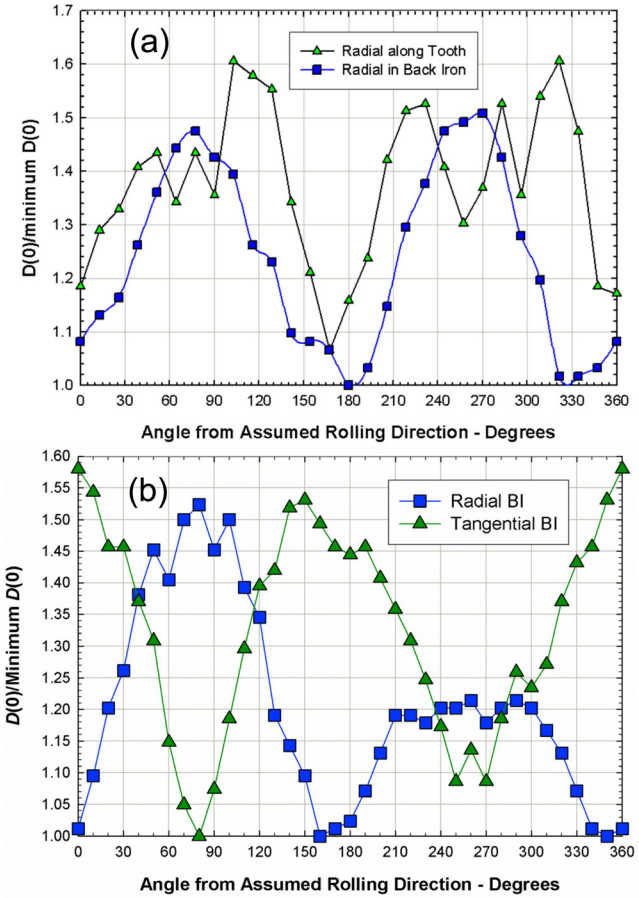

FIG. 4. (a) Comparison of $D(0)$ measurements in radial directions in the teeth and in the back iron region of an M36 rotor lamination. (b) Comparison of $D(0)$ measurements in the tangential and radial directions in the back iron region of an M36 stator lamination.

Fig. 3(a). The greater smoothness and symmetry between left and right halves of the M19 plot is conjectured to reflect lesser distortion of the textural anisotropy by the cutting in thinner material. Note the dip at 270° in the M36 in proximity to the keyway (KW). This is however not sensed in the M19 plot. Fig. 3(b) compares the radial and tangential measurements of $D(0)$ in the back iron region of a M19 rotor lamination. The clear 90° shift between these two plots evidences the dominance of texture, while the slightly lower peaks in the tangential plot seems to reflect the further distance of all points in a tangential stroke from cut edges. Significant differences are seen in the two data sets plotted in Fig. 4(a). Whereas the back iron plot shows only relatively small local departures from a texture related anisotropy, the tooth region data shows major departures from such a signature. The substantial differences in both the overall range and smoothness of point to point variations is deemed to reflect the expectedly greater distortion of the texture related anisotropy by the local deformations and stresses created when cutting the necessarily extensive tooth/slot edges. The high sensitivity of the $D(0)$ measurements to locally varying coercive forces are shown in Fig. 4(b). The 90° displacement between the major features (2 peaks and 2 valleys) of the plots of tangential and radial $D(0)$ measurements in the back iron region of an M36 stator lamination shown in Fig. 4(b) again attests (as with the plots in Fig. 3(b) of data from an M19 rotor lamination) to the domination of the roll induced texture in the sheet material. Seen in Fig. 4(b) however, is an asymmetry between the amplitude peaks of the radial data plots, and between the valley depths of the tangential data plots. Substantially this same asymmetry was found in all 4 of the M36 stator laminations, but was not seen in the M19 samples. The quantity $D(0)$ is obtained from measurements at a single point on each sample, always different from the location of every other data point. Repeatability of each measurement is typically within ±2%. Overall, the measurements show that maximum to minimum H_c ratios range between 1.4–1.7. This corresponds with TD-RD ratios reported by other authors, e.g., 1.7.[2] The presented methodology has the advantage to recover this ratio locally.

[1]P. Beckley, *Electrical Steels for Rotating Machines, Power and Energy Series* (IET, London, UK, 2002), pp. 122–124.
[2]M. Emura *et al.*, J. Magn. Magn. Mater. **226**, 1524 (2001).
[3]S. Urata *et al.*, IEEE Trans. Magn. **42**, 615 (2006).
[4]*Advanced Computer Techniques in Applied Electromagnetics* edited by M. H. Gracia and K. Hameyer (IOS Press, 2008).
[5]M. Emura *et al.*, J. Magn. Magn. Mater. **254**, 358 (2003).
[6]B. Hribernik, J. Magn. Magn. Mater. **26**, 72 (1982).
[7]I. J. Garshelis and G. Crevecoeur, J. Sens. **2012**, 870916.
[8]I. J. Garshelis and G. Crevecoeur, IEEE Trans. Magn. **48**, 4409 (2012).
[9]I. J. Garshelis *et al.*, J. Appl. Phys. **109**, 07E518 (2011).